

RD-R163 549

IFD (IMPLICIT FINITE-DIFFERENCE) WIDE ANGLE CAPABILITY
(U) NAVAL UNDERWATER SYSTEMS CENTER NEW LONDON CT NEW
LONDON LAB G BOTSEAS ET AL. 28 OCT 83 NUSC-TR-6905

1/1

UNCLASSIFIED

F/G 20/1

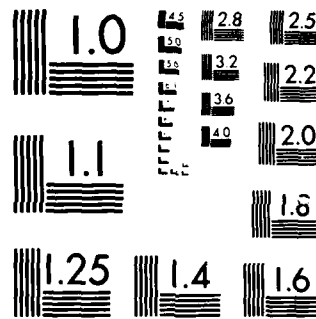
NL



END

FORMED

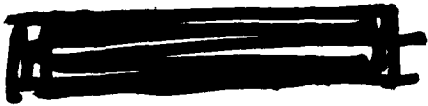
20



MICROCOPY RESOLUTION TEST CHART
NATIONAL BUREAU OF STANDARDS 1967 A

NUSC Technical Report 6905
28 October 1983

1



IFD: Wide Angle Capability

George Botseas
Ding Lee
Surface Ship Sonar Department

Kenneth E. Gilbert
Naval Ocean Research and
Development Activity
NSTL Station, MS 39529

DTIC
ELECTED
FEB 04 1986
S D

AD-A163 549



Naval Underwater Systems Center
Newport, Rhode Island / New London, Connecticut

100% FILE COPY

Approved for public release; distribution unlimited.

Preface

This report was prepared under two joint projects: (1) NUSC Project No. A65020, Finite-Difference Solutions to Acoustic Wave Propagation, Principal Investigator Dr. D. Lee, Code 3342. This portion was supported by NAVMAT, Program Manager CAPT D. F. Parrish, Code 08L, Program Element 61152N, Navy Sub/Task ZR00000101, *In-House Laboratory Research*, (2) NUSC Project No. A65021, *Parabolic Equation Applications*, Principal Investigator Dr. D. Lee, Code 3342 and Co-Investigator Dr. K. E. Gilbert, NORDA. This portion was supported by NORDA, Program Manager LCDR M. A. McCallister, Code 520, Program Element 63785N.

The technical reviewer for this report was Dr. A. H. Quazi, Code 3331.

Reviewed and Approved: 28 October 1983


W. A. Von Winkle
Associate Technical Director for Technology

The principal investigator of this report is located at the
New London Laboratory, Naval Underwater Systems Center,
New London, Connecticut 06320.

REPORT DOCUMENTATION PAGE		READ INSTRUCTIONS BEFORE COMPLETING FORM
1. REPORT NUMBER TR 6905	2. GOVT ACCESSION NO. <i>AD-A163 549</i>	3. RECIPIENT'S CATALOG NUMBER
4. TITLE (and Subtitle) IFD: WIDE ANGLE CAPABILITY	5. TYPE OF REPORT & PERIOD COVERED	
7. AUTHOR(S) George Botseas (NUSC) Ding Lee (NUSC) Kenneth E. Gilbert (NORDA)	8. PERFORMING ORG. REPORT NUMBER	
9. PERFORMING ORGANIZATION NAME AND ADDRESS Naval Underwater Systems Center New London Laboratory New London, Connecticut 06320	10. PROGRAM ELEMENT, PROJECT, TASK AREA & WORK UNIT NUMBERS A65020 61152N A65021	
11. CONTROLLING OFFICE NAME AND ADDRESS	12. REPORT DATE 28 October 1983	
	13. NUMBER OF PAGES 22	
14. MONITORING AGENCY NAME & ADDRESS (if different from Controlling Office)	15. SECURITY CLASS. (of this report) UNCLASSIFIED	
	15a. DECLASSIFICATION/DOWNGRADING SCHEDULE	
16. DISTRIBUTION STATEMENT (of this Report) Approved for public release; distribution unlimited.		
17. DISTRIBUTION STATEMENT (of the abstract entered in Block 20, if different from Report)		
18. SUPPLEMENTARY NOTES <i>1 2 3</i>		
19. KEY WORDS (Continue on reverse side if necessary and identify by block number) Computer model : Propagation loss Wide angle Implicit finite difference Range dependent Numerical methods Range independent Parabolic wave equation Underwater acoustics		
20. ABSTRACT (Continue on reverse side if necessary and identify by block number) In 1982, a general-purpose computer model, based on the implementation of an implicit finite-difference (IFD) scheme, was developed by Lee and Botseas at the Naval Underwater Systems Center (NUSC) for the solution of the parabolic-wave equation (PE). This model is being used to predict acoustic propagation loss in both range-dependent and range-independent environments. In this report, a recent improvement that extends the modeling of propagation angles from less than approximately 15 deg up to approximately 40 deg and the modifications that		

20. (Cont'd)

incorporate this improvement into the IFD model are presented. IFD calculations with and without this improvement are compared with normal-mode and fast-field-program (FFP) solutions for an isovelocity range-independent test case.

TABLE OF CONTENTS

	Page
1. INTRODUCTION	1
2. MATHEMATICAL FORMULATION	2
2.1 Horizontal-Interface Conditions	2
2.2 Two-Way Farfield Equation With Interface Conditions	3
2.3 Improved Parabolic Equation	5
2.4 Wide-Angle Capability	9
3. COMPUTER IMPLEMENTATION	9
3.1 Input Format	9
3.2 Output Format	13
4. TEST PROBLEM	15
5. CONCLUSIONS	17
REFERENCES	18

LIST OF ILLUSTRATIONS

Figure	Page
1 The Interface Between Two Media	2
2 Comparison of MODE (SNAP) and FFP Results for Test Case 3B	16
3 Comparison of Wide-Angle and Standard Tappert PE Solutions	16

Accession For	
NTIS CRA&I	<input checked="" type="checkbox"/>
DTIC TAB	<input type="checkbox"/>
Unannounced	<input type="checkbox"/>
Justification	
By	
Distribution/	
Availability Codes	
Dist	Available and/or Special
A-1	

IFD: WIDE-ANGLE CAPABILITY

1. INTRODUCTION

A useful approach for calculating underwater-sound propagation in a range-dependent environment was introduced by Tappert,¹⁻⁴ who used a parabolic-equation (PE) method to solve the acoustic wave equation. Tappert's PE approximation transforms the acoustic wave equation, which is an elliptic partial-differential equation, into a parabolic partial-differential equation. The resulting PE governs the outgoing field and can be solved by the split-step Fourier algorithm developed by Tappert. The split-step algorithm solves the parabolic wave equation by imposing an artificial zero bottom-boundary condition and pressure-release surface condition; therefore, it solves a pure initial-value problem. In cases where bottom interaction is strong, a more general-purpose solution is useful for handling a bottom-boundary condition. For this reason, Lee, Botseas, and Papadakis^{5,6} developed an implicit finite-difference (IFD) scheme as well as an ordinary-differential (ODE) method to solve Tappert's parabolic wave equation. Their schemes are designed to treat the bottom-boundary condition exactly. Carnahan's⁷ approach in handling the horizontal-interface boundary condition for the heat-transfer problem was used by McDaniel and Lee⁸ to incorporate interface conditions into the parabolic wave equation.

These interface conditions were programmed into the IFD computer model by Lee and Botseas.⁹ Since then, Gilbert¹⁰ and Greenell derived an improved equation that extends the treatment of propagation angles in Tappert's equation from less than approximately 15 deg up to approximately 40 deg. For wide-angle (>15 deg) propagation, Tappert's original equation can introduce large phase errors into the solution; furthermore, it is with wide-angle propagation that strong bottom interaction generally takes place. Consequently, accurate treatment of bottom-boundary conditions and wide-angle propagation are closely related problems. Recent progress in the theory, development, and implementation of a wide-angle PE is reported in references 12 and 13. The incorporation of the wide-angle capability into the IFD model is the topic of this report.

The mathematical formulation and modifications that incorporate the wide-angle capability into the IFD model are given in the next section. The same approach used by McDaniel and Lee⁸ is used to incorporate the interface conditions into the improved wide-angle parabolic equation. Section 3 describes input and output formats in detail, while section 4 is devoted to a test problem.

External users can obtain a copy of the improved model by forwarding a formal request and a blank magnetic tape to the Naval Underwater Systems Center (NUSC). All programs are written in FORTRAN for the VAX-11/780 computer.

It is requested that the authors be notified if any difficulties with the model are experienced. User contributions that will enhance the model are invited.

2. MATHEMATICAL FORMULATION

The derivation of the improved wide-angle parabolic equation is presented in four parts. First, McDaniel and Lee's⁸ discussion on horizontal-interface conditions that apply to the two-way (outgoing and incoming) farfield equation is presented. Second, McDaniel and Lee's⁸ procedure is used to incorporate these interface conditions into the two-way farfield equation for the acoustic field. Third, the farfield equation with interface conditions is formally solved, resulting in an improved one-way outgoing wave equation. Finally, the coefficients that give the improved equation wide-angle capability are presented.

2.1 HORIZONTAL-INTERFACE CONDITIONS

Consider two different media, as shown in figure 1, in which a numerical subscript indicates the medium, and z_B is the interface depth. Let ρ be a constant density, and let p be the acoustic pressure. For a cylindrically symmetric geometry and a harmonic source, p satisfies the reduced wave equation

$$\nabla^2 p + k_0^2 n^2(r, z) p = 0 , \quad (2-1)$$

where k_0 is a reference wavenumber and $n(r, z)$ is the index of refraction. We substitute

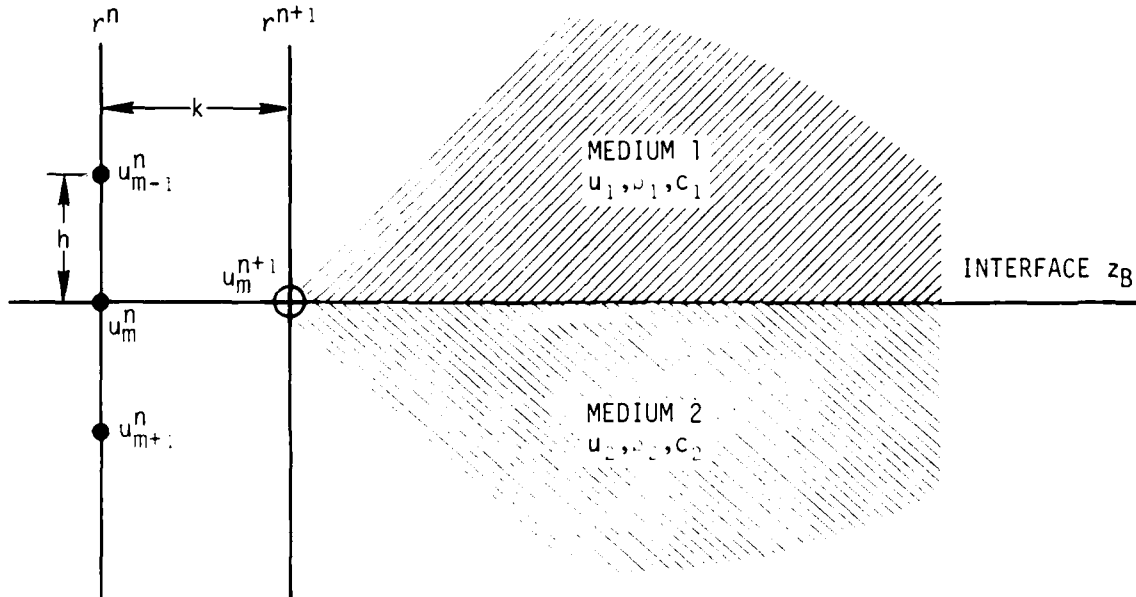


Figure 1. The Interface Between Two Media

$$p(r, z) = u(r, z) H_0^{(1)}(k_0 r), \quad (2-2)$$

into equation (2-1). The result obtained is the two-way (outgoing and incoming) farfield equation for the acoustic field, u ,

$$u_{rr} + 2ik_0 u_r + k_0^2(n^2 - 1)u + u_{zz} = 0. \quad (2-3)$$

We seek boundary conditions for a horizontal interface that apply to equation (2-3).

The continuity of pressure gives rise to the first interface condition,

$$p_1(r, z_B) = p_2(r, z_B). \quad (2-4)$$

The continuity of the normal component of particle velocity gives rise to the second interface condition,

$$\rho_2 \left. \frac{\partial p_1}{\partial z} \right|_{z_B} = \rho_1 \left. \frac{\partial p_2}{\partial z} \right|_{z_B}. \quad (2-5)$$

By substituting equation (2-2) into equation (2-4), we obtain the first interface condition for the parabolic wave equation,

$$u_1(r, z_B) = u_2(r, z_B). \quad (2-6)$$

Taking partial derivatives of both sides of equation (2-2) with respect to z and substituting the results into equation (2-5), we obtain the second interface condition for the parabolic wave equation,

$$\rho_2 \left. \frac{\partial u_1}{\partial z} \right|_{z_B} = \rho_1 \left. \frac{\partial u_2}{\partial z} \right|_{z_B}. \quad (2-7)$$

2.2 TWO-WAY FARFIELD EQUATION WITH INTERFACE CONDITIONS

The treatment to be discussed in this section deals with a horizontal fluid boundary. A uniform partition in the z direction is assumed, with $\Delta z = h$. The range increment Δr is denoted by k , and m is an integer index that indicates the interface boundary. Superscripts indicate the range level and subscripts indicate the depth level. We use the convention that if both the superscript and subscript are dropped, the field denotes the field at (nk, mh) , i.e., $u = u_m^n$.

Consider the case shown in figure 1, where u_m^n denotes the field at $z = m(\Delta z) = mh$, $r = n(\Delta r) = nk$. Our main effort is to determine u_m^{n+1} such that the conditions imposed by equations (2-6) and (2-7) are satisfied.

Medium 1

In medium 1, the field must satisfy equation (2-3), i.e.,

$$(u_1)_{rr} + 2ik_0(u_1)_r + k_0^2(n_1^2 - 1)u_1 + (u_1)_{zz} = 0 \quad (2-8)$$

Using the first three terms of a Taylor series expansion for u_{m-1}^n upon u_m^n and solving for u_{zz} , we find

$$\frac{\partial^2 u_1}{\partial z^2} = -\frac{2}{h^2}(u_1 - u_{m-1}^n) + \frac{2}{h} \times \frac{\partial u_1}{\partial z}. \quad (2-9)$$

Substituting equation (2-9) into equation (2-8) and simplifying, we obtain

$$\frac{\partial u_1}{\partial z} = -\frac{h}{2} \left\{ \frac{\partial^2 u_1}{\partial r^2} + 2ik_0 \frac{\partial u_1}{\partial r} + k_0^2(n_1^2 - 1)u_1 + \left[-\frac{2}{h^2}(u_1 - u_{m-1}^n) \right] \right\}. \quad (2-10)$$

Medium 2

Similarly, in medium 2, the field must satisfy equation (2-3), i.e.,

$$(u_2)_{rr} + 2ik_0(u_2)_r + k_0^2(n_2^2 - 1)u_2 + (u_2)_{zz} = 0. \quad (2-11)$$

Using the first three terms of a Taylor series expansion for u_{m+1}^n upon u_m^n and solving for u_{zz} , we find

$$\frac{\partial^2 u_2}{\partial z^2} = \frac{2}{h^2}(u_{m+1}^n - u_2) - \frac{2}{h} \times \frac{\partial u_2}{\partial z}. \quad (2-12)$$

Substituting equation (2-12) into equation (2-11) and simplifying, we obtain

$$\frac{\partial u_2}{\partial z} = \frac{h}{2} \left\{ \frac{\partial^2 u_2}{\partial r^2} + 2ik_0 \frac{\partial u_2}{\partial r} + k_0^2(n_2^2 - 1)u_2 + \left[\frac{2}{h^2}(u_{m+1}^n - u_2) \right] \right\}. \quad (2-13)$$

In view of the first interface condition, equation (2-6), we require that $u_1 = u_2 = u$ in equations (2-10) and (2-13). Then, we multiply both sides of equation (2-10) by ρ_2 and both sides of equation (2-13) by ρ_1 and equate the results, using the second interface condition, equation (2-7). After simplifying, we obtain the following parabolic equation:

$$\begin{aligned} u_{rr} + 2ik_0 u_r + \frac{\rho_1}{\rho_1 + \rho_2} \left(k_2^2 + \frac{\rho_2}{\rho_1} k_1^2 \right) u - k_0^2 u \\ + \frac{2\rho_2}{h^2(\rho_1 + \rho_2)} \left(u_{m-1}^n - \frac{\rho_1 + \rho_2}{\rho_2} u + \frac{\rho_1}{\rho_2} u_{m+1}^n \right) = 0. \end{aligned} \quad (2-14)$$

Equation (2-14) is the parabolic wave equation satisfied by the field u on the interface z_B . Note that $c_1(r, z) = c_2(r, z)$ implies that $k_1 = k_2$. If, in addition, $\rho_1 = \rho_2$, equation (2-14) reduces to

$$u_{rr} + 2ik_0 u_r + k_0^2(n^2 - 1)u + \frac{(u_{m+1}^n - u_m^n) - (u_m^n - u_{m-1}^n)}{h^2} = 0. \quad (2-15)$$

Regarding

$$h^{-2} [(u_{m+1}^n - u_m^n) - (u_m^n - u_{m-1}^n)]$$

as the central finite-difference operator for u_{zz} , equation (2-15) becomes exactly the parabolic wave equation, equation (2-3), in one medium. Next, define

$$\tau_{zz}^n u = \frac{2\rho_2}{h^2(\rho_1 + \rho_2)} \left(u_{m-1} - \frac{\rho_1 + \rho_2}{\rho_2} u + \frac{\rho_1}{\rho_2} u_{m+1} \right) \quad (2-16)$$

and

$$G = \frac{\rho_1}{\rho_1 + \rho_2} \left(k_2^2 + \frac{\rho_2}{\rho_1} k_1^2 \right) - k_0^2 + \tau_{zz}, \quad (2-17)$$

and rewrite equation (2-14) as

$$u_{rr} + 2ik_0 u_r + Gu = 0. \quad (2-18)$$

Equation (2-18) is the two-way farfield equation with interface conditions for the acoustic field.

2.3 IMPROVED PARABOLIC EQUATION

The associated one-way outgoing wave equation is obtained by using the quadratic equation formula to formally solve equation (2-18) for $\partial u / \partial r$,

$$\partial u / \partial r = +i(\sqrt{k_0^2 + G} - k_0)u. \quad (2-19)$$

In equation (2-19), the plus sign has been chosen so that outgoing waves are represented. For a range-independent medium, equation (2-19) is exact, that is, a solution of equation (2-19) is also a solution of equation (2-3). Now, write

$$Q = k_0^2 + G. \quad (2-20)$$

Equation (2-19) can now be written as

$$\partial u / \partial r = i(\sqrt{Q} - k_0)u. \quad (2-21)$$

Now write

$$Q = k_0^2 \left(\frac{Q}{k_0^2} + 1 - 1 \right) , \quad (2-22)$$

define

$$q = \frac{Q}{k_0^2} - 1 , \quad (2-23)$$

and rewrite

$$Q = k_0^2(q + 1) . \quad (2-24)$$

Using a rational function approximation for the square root operator

$$\sqrt{Q} = k_0 \left(\frac{A + Bq}{C + Dq} \right) \quad (2-25)$$

and substituting equation (2-25) into equation (2-21), we find that

$$\frac{\partial u}{\partial r} = ik_0 \left(\frac{A + Bq}{C + Dq} - 1 \right) u . \quad (2-26)$$

Rewriting equation (2-26), we have

$$(C + Dq) \frac{\partial u}{\partial r} u = ik_0 [(A - C) + (B - D)q] u . \quad (2-27)$$

Assuming Q is a constant over the interval r^n and r^{n+1} and using the Crank-Nicolson scheme to solve equation (2-21), we find that

$$u^{n+1} - u^n = i \left(\sqrt{Q} - k_0 \right) \left(\frac{u^{n+1} + u^n}{2} \right) \Delta r , \quad (2-28)$$

where $\Delta r = r^{n+1} - r^n$. The resulting implicit equation is

$$\left[1 - i \left(\sqrt{Q} - k_0 \right) \frac{\Delta r}{2} \right] u^{n+1} = \left[1 + i \left(\sqrt{Q} - k_0 \right) \frac{\Delta r}{2} \right] u^n . \quad (2-29)$$

Using the definition for Q along with the rational approximation for Q , we obtain

$$\left[1 - ik_0 \left(\frac{A + B \frac{G}{k_0^2}}{C + D \frac{G}{k_0^2}} - 1 \right) \frac{\Delta r}{2} \right] u^{n+1} = \left[1 + ik_0 \left(\frac{A + B \frac{G}{k_0^2}}{C + D \frac{G}{k_0^2}} - 1 \right) \frac{\Delta r}{2} \right] u^n . \quad (2-30)$$

Substituting equation (2-17) into equation (2-30) and simplifying, we have

$$\begin{aligned}
& \left[C + D \left\{ \frac{\rho_1}{\rho_1 + \rho_2} \left(n_2^2 + \frac{\rho_2}{\rho_1} n_1^2 \right) - 1 \right\} - ik_0 \left\{ A - C + (B - D) \left[\frac{\rho_1}{\rho_1 + \rho_2} \left(n_2^2 \right. \right. \right. \right. \\
& \left. \left. \left. \left. + \frac{\rho_2}{\rho_1} n_1^2 \right) - 1 \right] \right\} \frac{\Delta r}{2} + \frac{1}{k_0^2} \left[D - ik_0 (B - D) \frac{\Delta r}{2} \right] \tau_{zz} u^{n+1} \right. \\
& = C + D \left[\frac{\rho_1}{\rho_1 + \rho_2} \left(n_2^2 + \frac{\rho_2}{\rho_1} n_1^2 \right) - 1 \right] + ik_0 \left\{ A - C + (B - D) \left[\frac{\rho_1}{\rho_1 + \rho_2} \left(n_2^2 \right. \right. \right. \right. \\
& \left. \left. \left. \left. + \frac{\rho_2}{\rho_1} n_1^2 \right) - 1 \right] \right\} \frac{\Delta r}{2} + \frac{1}{k_0^2} \left[D + ik_0 (B - D) \frac{\Delta r}{2} \right] \tau_{zz} \left. u^n \right] . \tag{2-31}
\end{aligned}$$

Now, define

$$n = \frac{\rho_1}{\rho_1 + \rho_2} \left(n_2^2 + \frac{\rho_2}{\rho_1} n_1^2 \right) - 1 \tag{2-32}$$

and substitute equation (2-16) into equation (2-31). We now have

$$\begin{aligned}
& u_m^{n+1} \left\{ C + Dn - ik_0 [(A - C) + (B - D)n] \frac{\Delta r}{2} \right\} + \frac{1}{k_0^2} \left[D - ik_0 (B - D) \frac{\Delta r}{2} \right] \\
& \cdot \frac{2\rho_2}{(\Delta z)^2 (\rho_1 + \rho_2)} \left(u_{m-1}^{n+1} - \frac{\rho_1 + \rho_2}{\rho_2} u_m^{n+1} + \frac{\rho_1}{\rho_2} u_{m+1}^{n+1} \right) \\
& = u_m^n \left\{ C + Dn + ik_0 [(A - C) + (B - D)n] \frac{\Delta r}{2} \right\} + \frac{1}{k_0^2} \left[D + ik_0 (B - D) \frac{\Delta r}{2} \right] \\
& \cdot \frac{2\rho_2}{(\Delta z)^2 (\rho_1 + \rho_2)} \left(u_{m-1}^n - \frac{\rho_1 + \rho_2}{\rho_2} u_m^n + \frac{\rho_1}{\rho_2} u_{m+1}^n \right) . \tag{2-33}
\end{aligned}$$

Next, define

$$W_1 = C + \frac{ik_0 \Delta r}{2} (A - C) \tag{2-34}$$

$$W_1^* = C - \frac{ik_0 \Delta r}{2} (A - C) \tag{2-35}$$

$$W_2 = D + \frac{ik_0 \Delta r}{2} (B - D) \tag{2-36}$$

and

$$W_2^* = D - \frac{ik_0 \Delta r}{2}(B - D) \quad (2-37)$$

Substituting equations (2-34) to (2-37) into equation (2-33) and simplifying, we have

$$\begin{aligned} & \left(\frac{W_1^*}{W_2^*} + \eta \right) u_m^{n+1} + \frac{1}{k_0^2} \left[\frac{2\rho_2}{(\Delta z)^2(\rho_1 + \rho_2)} \right] \left(u_{m-1}^{n+1} - \frac{\rho_1 + \rho_2}{\rho_2} u_m^{n+1} + \frac{\rho_1}{\rho_2} u_{m+1}^{n+1} \right) \\ &= \left(\frac{W_1 + W_2 n}{W_2^*} \right) u_m^n + \frac{1}{k_0^2} \left(\frac{W_2}{W_2^*} \right) \left[\frac{2\rho_2}{(\Delta z)^2(\rho_1 + \rho_2)} \right] \left(u_{m-1}^n - \frac{\rho_1 + \rho_2}{\rho_2} u_m^n + \frac{\rho_1}{\rho_2} u_{m+1}^n \right) \quad (2-38) \end{aligned}$$

Multiplying by $k_0^2(\Delta z)^2(\rho_1 + \rho_2)/2\rho_2$ results in

$$\begin{aligned} & \left(\frac{W_1^*}{W_2^*} + \eta \right) \frac{k_0^2(\Delta z)^2(\rho_1 + \rho_2)}{2\rho_2} u_m^{n+1} + \left(u_{m-1}^{n+1} - \frac{\rho_1 + \rho_2}{\rho_2} u_m^{n+1} + \frac{\rho_1}{\rho_2} u_{m+1}^{n+1} \right) \\ &= \left(\frac{W_1 + W_2 n}{W_2^*} \right) \frac{k_0^2(\Delta z)^2(\rho_1 + \rho_2)}{2\rho_2} u_m^n + \frac{W_2}{W_2^*} \left(u_{m-1}^n - \frac{\rho_1 + \rho_2}{\rho_2} u_m^n + \frac{\rho_1}{\rho_2} u_{m+1}^n \right) \quad (2-39) \end{aligned}$$

Substituting equation (2-32) into equation (2-39) and regrouping terms gives

$$\begin{aligned} u_{m-1} + \left\{ \left(\frac{W_1^*}{W_2^*} \right) \frac{k_0^2(\Delta z)^2(\rho_1 + \rho_2)}{2\rho_2} - \frac{\rho_1 + \rho_2}{\rho_2} + \frac{(\Delta z)^2 k_0^2}{2} \left[\frac{\rho_1}{\rho_2} \left(n_2^2 - 1 \right) + \left(n_1^2 - 1 \right) \right] \right\} u_m^{n+1} + \frac{\rho_1}{\rho_2} u_{m+1}^{n+1} &= \left(\frac{W_2}{W_2^*} \right) u_{m-1} + \left\{ \left(\frac{W_1^*}{W_2^*} \right) \frac{k_0^2(\Delta z)^2(\rho_1 + \rho_2)}{2\rho_2} - \left(\frac{W_2}{W_2^*} \right) \right. \\ &\quad \left. \times \frac{\rho_1 + \rho_2}{\rho_2} + \left(\frac{W_2}{W_2^*} \right) \frac{(\Delta z)^2 k_0^2}{2} \left[\frac{\rho_1}{\rho_2} \left(n_2^2 - 1 \right) + \left(n_1^2 - 1 \right) \right] \right\} u_m^n + \frac{\rho_1}{\rho_2} \left(\frac{W_2}{W_2^*} \right) u_{m+1}^n \quad (2-40) \end{aligned}$$

In a matrix form, equation (2-40) becomes

$$\begin{aligned} \left[1, \left(\frac{W_1^*}{W_2^*} \right) \frac{k_0^2(\Delta z)^2(\rho_1 + \rho_2)}{2\rho_2} - \frac{\rho_1 + \rho_2}{\rho_2} + \frac{(\Delta z)^2 k_0^2}{2} \left[\frac{\rho_1}{\rho_2} \left(n_2^2 - 1 \right) + \left(n_1^2 - 1 \right) \right] - 1 \right], \frac{\rho_1}{\rho_2} \begin{pmatrix} u_{m-1}^{n+1} \\ u_m^{n+1} \\ u_{m+1}^{n+1} \end{pmatrix} &= \left\{ \frac{W_2}{W_2^*}, \left(\frac{W_1^*}{W_2^*} \right) \frac{k_0^2(\Delta z)^2(\rho_1 + \rho_2)}{2\rho_2} - \left(\frac{W_2}{W_2^*} \right) \frac{\rho_1 + \rho_2}{2} \right\} \quad (2-41) \end{aligned}$$

$$+ \left(\frac{W_2}{W_2^*} \right) \frac{(\Delta z)^2 k^2}{2} \left[\frac{\rho_1}{\rho_2} \left(n_2^2 - 1 \right) + \left(n_1^2 - 1 \right) \right], \frac{\rho_1 W_2}{\rho_2 W_2^*} \begin{pmatrix} u_{m-1}^n \\ u_m^n \\ u_{m+1}^n \end{pmatrix} .$$

Only simple modifications were required to incorporate the improved PE and horizontal interface conditions into the IFD model.⁹

2.4 WIDE-ANGLE CAPABILITY

The capability to handle wider propagation angles results from judicious selection of the coefficients, A, B, C, and D in the rational function approximation for the square root operator in equation (2-25).¹³

If we select A = 1, B = 1/2, C = 1, and D = 0, equation (2-41) reduces to a solution of the standard Tappert parabolic equation. Tappert's equation is limited to propagation angles of less than approximately 15 deg.

Claerbout's^{14,15} one-way equation uses A = 1, B = 3/4, C = 1, and D = 1/4. Claerbout's coefficients extend the propagation angle to approximately 40 deg. Claerbout's approximation is equivalent to a quadratic expansion of \sqrt{Q} , whereas Tappert's approximation is a linear expansion.

3. COMPUTER IMPLEMENTATION

The model that implements the implicit finite-difference (IFD) formula, equation (2-41), has been written in FORTRAN using single-precision complex arithmetic and has been installed on a VAX-11/780 digital computer. For a detailed description of the IFD model, the reader is referred to reference 9.

The next two subsections describe input and output formats in detail. The only difference in formats between this and the original IFD model is in the insertion of card 2A into the input runstream. Test examples showing a variety of sample input runstreams and user-written subroutines can be found in reference 9. To rerun those test examples, card 2A must be inserted in the runstream.

3.1 INPUT FORMAT

Prior to executing the IFD model, input card images containing problem parameters must be stored in file IFD.IN. File IFD.IN is assigned to FORTRAN unit number NIU in the main program. If the user prefers to input problem parameters on cards, then parameter NIU should be equated to the card reader unit number, and the statement that assigns file IFD.IN should be removed from the main program. In either case, the input runstream is prepared in free format as follows.

<u>CARD</u>	<u>CONTENTS</u>
-------------	-----------------

1	FRQ, ZS, CO, ISF, RA, ZA, N, IHNK, ITYPEB, ITYPES
---	---

where

FRQ = frequency (Hz).

ZS = source depth (m).

CO = reference sound speed (m/s).

If CO = 0.0, CO is set to the average sound speed in the first layer.

ISF = starting field flag.

0 = Gaussian starting field is generated.

1 = user prepares starting field. See subroutine UFIELD.

If ISF = 0, RA is set to zero.

RA = horizontal range from source to starting field (m).

If ISF = 0, RA is set to 0.0.

ZA = depth of starting field at range RA (m). If ZA = 0.0, ZA is set to the maximum depth of the bottommost layer in the first profile.

If ITYPEB = 2 or 3 and ZA = 0.0, ZA is set to $(4/3)^*$ maximum depth of the bottommost layer. If ITYPEB = 2 or 3 and ZA \neq 0.0, the artificial bottom layer is extended to ZA meters provided that ZA is greater than or equal to the maximum depth of the bottommost layer in the first profile.

N = number of equispaced receivers in the starting field. If N = 0, N is set so that the receiver depth increment is less than or equal to 1/4 wavelength. If N is greater than MXN, N is set to MXN. See parameter MXN.

IHNK = Hankel function flag. If IHNK = 0, don't use Hankel function. If IHNK = 1, divide the starting field by the Hankel function, then multiply the solution field by the Hankel function before computing propagation loss. If starting field is Gaussian, IHNK should be set to 0. If starting field is elliptic, IHNK should be set to 1.

ITYPEB = type of bottom.

= 0, homogeneous Neumann boundary condition; program supplies bottom condition.

CARDCONTENTS

= 1, user supplies bottom condition. See subroutine BCON.
 = 2, artificial absorbing layer introduced; bottom of layer follows contour of water-bottom interface.
 = 3, artificial absorbing layer introduced; bottom of layer kept flat.

ITYPES = type of surface.

= 0, pressure release; SCON sets SURY and SURX = 0.0.
 ≠ 0, user inserts code in SCON to compute SURY and SURX.

2 RMAX, DR, WDR, WDZ, PDR, PDZ, ISFLD, ISVP, IBOT

where

RMAX = maximum range of solution (m).
 DR = range step for marching solution (m).
 If DR = 0, DR is set to 1/2 wavelength.
 WDR = range step (rounded to nearest DR) at which solution is written on disk (m).
 WDZ = depth increment (rounded to nearest DZ) at which solution is written on disk (m).
 PDR = range step (rounded to nearest DR) at which solution is printed (m).
 PDZ = depth increment (rounded to nearest DZ) at which solution is printed (m).
 ISFLD = 0, don't print starting field.
 = 1, print starting field.
 ISVP = 0, don't print sound-speed profile.
 = 1, print sound-speed profile.
 IBOT = 0, don't print bottom depths.
 = 1, print bottom depths.

2A A, B, C, D

TAPPERT: A = 1, B = 0.5, C = 1, and D = 0.

CARD CONTENTSCLAERBOUT: $A = 1.0$, $B = 0.75$, $C = 1.0$, and $D = 0.25$.

3	R1, Z1	}	Bottom profile. Range and depth of water (m); maximum number of depths = 100 (see parameter MXTRK).
4	R2, Z2		
5	R3, Z3		
.	.		
.	.		
N	.		
N+1	-1, -1	Required. Marks end of bottom profile.	
N+2	RSVP	}	Repeat for each profile.
N+3	KSVP		
N+4	NLYR		
N+5	ZLYR(I), RHO(I), BETA(I)		
N+6	ZSVP(1), CSVP(1)		
N+7	ZSVP(2), CSVP(2)		
.	.		
.	.		
N+M	ZSVP(J), CSVP(J)		
.	.		

where

RSVP = range of SVP (m).

KSVP = SVP flag.

= 0, profile is in runstream.

0, profile (cards N+4 through N+M) is supplied by user-written subroutine USVP. KSVP may be used in computed GOTO statement to transfer control in user subroutine USVP.

NLYR = number of layers. If ITYPEB = 2 or 3, the program inserts an artificial absorbing layer and then increments NLYR by 1. Maximum NLYR = 100 (see parameter MXLYR).

ZLYR(I) = maximum depth of layer I in profile (m).

CARDCONTENTS

RHO(I) = density in layer I (g/cm³).

BETA(I) = attenuation in layer I (dB/wavelength).

ZSVP = SVP depth (m). Maximum number of sound-speed profile values = 100 (see parameter MXSVP).

ZSVP(1) = depth to top of layer I (m).

ZSVP(J) = depth to bottom of layer I (m).

CSVP = SVP speed (m/s). Maximum number of sound-speed profile values = 100 (see parameter MXSVP).

CSVP(1) = speed of sound at top of layer I (m/s).

CSVP(J) = speed of sound at bottom of layer I (m/s).

3.2 OUTPUT FORMAT

Output from the IFD model is written on disk in file IFD.OUT. File IFD.OUT is assigned to FORTRAN unit number NOU in the main program. The data written in IFD.OUT are unformatted and are written with FORTRAN WRITE statements as follows.

```
WRITE(NOU)FRQ,ZS,CO,ISF,RA,ZA,N,IHNK,ITYPEB,ITYPES,RMAX,DR,WDR,DZ,  
NLYR,ZLYR,RHO,BETA.
```

```
WRITE(NOU)NZ,RA,WDZ,(U(I),I=IWZ,N,IWZ).
```

The first WRITE statement is executed only once and writes the value of each of the following parameters at the start of the problem.

FRQ = frequency (Hz).

ZS = source depth (m).

CO = reference sound speed (m/s).

ISF = starting field flag.

 = 0, Gaussian.

 = 1, user.

RA = horizontal range from source to starting field (m).

ZA = depth of starting field (m).

N = number of equispaced receivers in the starting field.

IHNK = Hankel function flag.
= 0, Hankel function not used.
= 1, starting field was divided by Hankel function.

ITYPEB = type of bottom.
= 0, rigid.
= 1, user bottom.
= 2, artificial absorbing layer, follows bottom contour.
= 3, artificial absorbing layer, bottom kept flat.

ITYPES = type of surface.
= 0, pressure release.
≠ 0, user supplied.

RMAX = maximum range of solution (m).

DR = range step for marching solution (m).

WDR = range step at which solution is written on disk (m).

DZ = depth increment of receivers (m).

NLYR = number of layers.

ZLYR = array containing depth of each layer (m).

RHO = array containing density in each layer (g/cm³).

BETA = array containing attenuation in each layer (dB/wavelength).

The second WRITE statement is executed at each write-range increment, WDR. The data written are as follows:

NZ = number of equispaced receivers in the solution field.

RA = horizontal range from source to solution (m).

WDZ = depth increment at which solution is written on disk (m).

U = array that contains the complex field at range RA.
If IHNK = 1, then the contents of U must be multiplied by the Hankel function before computing propagation loss.

IWZ = index increment of receiver solutions to be written on disk.

The following READ statement may be used to read the solution field:

```
READ(unit) NZ,RA,WDZ,(U(I)I=1,NZ).
```

4. TEST PROBLEM

The new IFD model with wide-angle capability is tested with test case 3B, extracted from reference 16. The environment for this case is range-independent and consists of an isovelocity water column over an isovelocity half-space bottom. Parameters for the problem are given below:

Frequency = 250 Hz,
Water depth = 100 m,
Sound speed in water = 1500 m/s,
Density in water = 1.0 g/cm³,
Density in bottom = 1.2 g/cm³,
Attenuation in water = 0,
Bottom attenuation = 0.5 dB/λ,
Bottom sound speed = 1590 m/s,
Maximum range = 10 km,
Source depth = 99.5 m,
Receiver depth = 99.5 m, and
Modes = 11.

With the source and receiver just off the bottom, the higher modes are more strongly excited, and all 11 modes are required for an accurate solution in the 5 to 10 km range interval. This, in turn, requires a half-beamwidth capability of 18.5 deg.

Comparisons with normal-mode results indicate that the fast-field program (FFP) solution shown in figure 2 is correct.^{11,17}

Two IFD solutions to test case 3B were obtained, one using Claerbout's coefficients A = 1, B = 3/4, C = 1, and D = 1/4 (wide-angle PE), and the other using the coefficients A = 1, B = 1/2, C = 1, and D = 0 (standard Tapert PE). In each case, a Gaussian pressure distribution and an artificial boundary extended to 250 m in depth were assumed. As shown in figure 3, the IFD solution obtained using Claerbout's coefficients differs slightly in level but, in general, is in excellent agreement with the FFP solution. The average level of the IFD solution to the standard PE is in good agreement with the FFP but the pattern of the solution is poor.

TR 6905

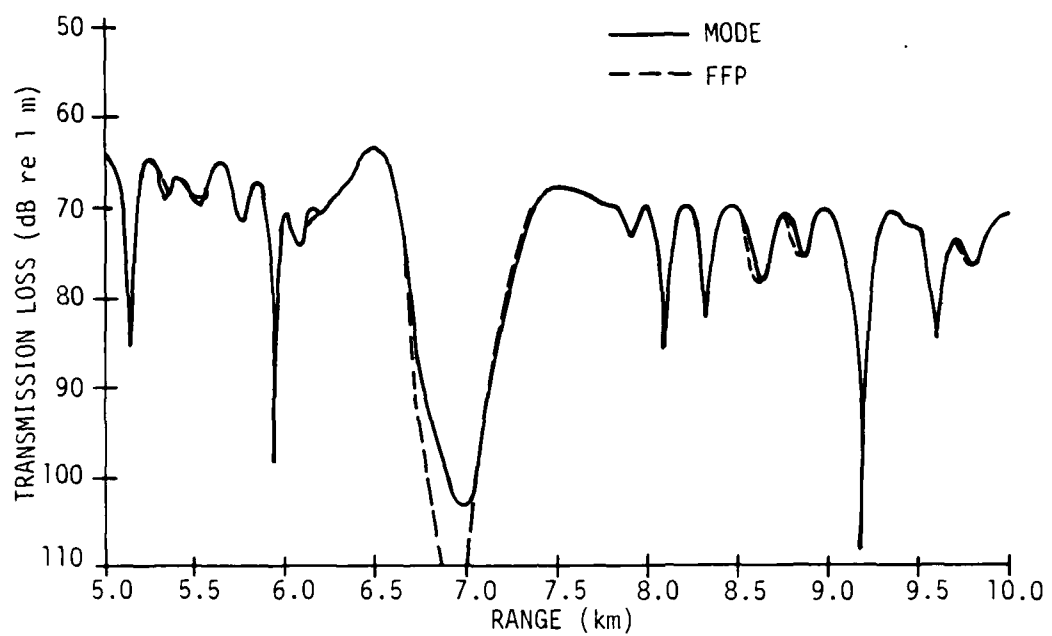


Figure 2. Comparison of MODE (SNAP) and FFP Results for Test Case 3B

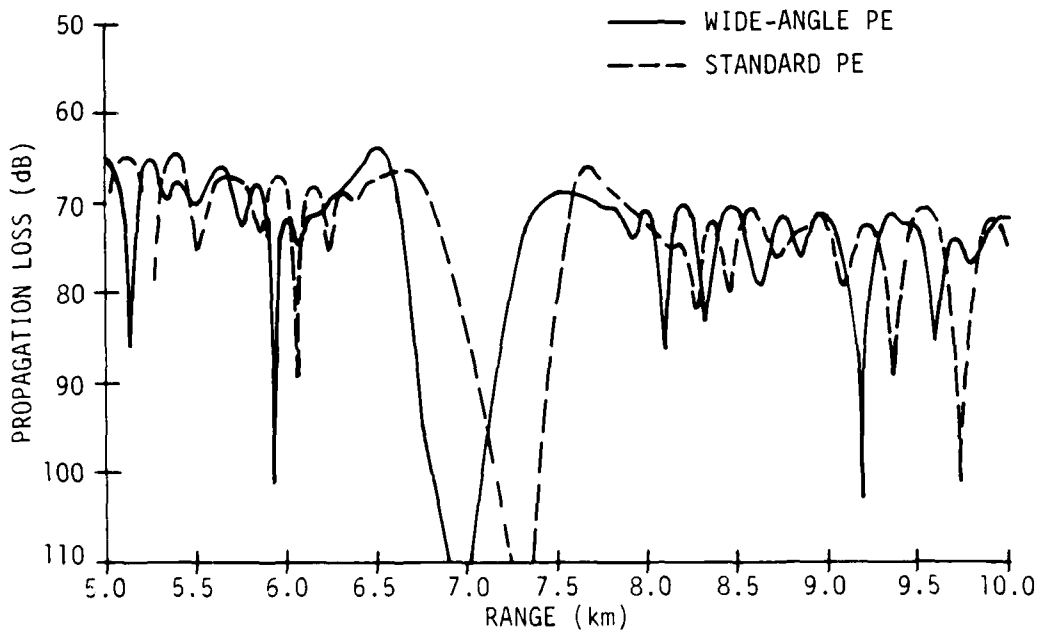


Figure 3. Comparison of Wide-Angle and Standard Tappert PE Solutions

The input runstream for test case 3B is listed below:

```
250 99.5 0 0 0 250 1000 0 3 0
10000 1 2 99.5 1000 20 0 0 0
1 .75 1 .25
0 100
10001 100
-1, -1
0
0
2
100 1 0
0 1500
100 1500
200 1.2 0.5
100 1590
200 1590
```

5. CONCLUSIONS

The mathematical formulation of a recent improvement that extends the modeling of propagation angles from less than approximately 15 deg up to approximately 40 deg and the modifications that incorporate this wide-angle capability into the IFD model were presented.

IFD calculations with and without the wide-angle capability were compared with normal-mode and FFP solutions for an isovelocity range-independent test case. IFD calculations obtained with the wide-angle improvement are in excellent agreement with the normal-mode and FFP solutions, whereas IFD calculations obtained without the improvement are subject to phase errors.

As demonstrated in this report, the capability to handle wide-angle propagation was incorporated into the IFD model quite easily. Future capabilities to be built into the model include multiple irregular interfaces, automatic step-size determination, high-frequency propagation, shear waves, and others.

REFERENCES

1. F. D. Tappert and R. H. Hardin, "Application of the Split-Step Fourier Method to the Numerical Solution of Nonlinear and Variable-Coefficient Wave Equations," Society for Industrial and Applied Mathematics (SIAM), rev. 15, 1973, p. 423.
2. F. D. Tappert and R. H. Hardin, A Synopsis of the AESD Workshop on Acoustic Modeling by Non-Ray Tracing Techniques, C. W. Spofford, AESD TN-73-05, Acoustic Environmental Support Detachment, Office of Naval Research, Arlington, VA, 1973.
3. F. D. Tappert and R. H. Hardin, "Computer Simulation of Long-Range Ocean Acoustic Propagation Using the Parabolic Equation Method," Eighth International Congress on Acoustics, London, England, 1974, p. 452.
4. F. D. Tappert, "The Parabolic Approximation Method," Wave Propagation and Underwater Acoustics, edited by J. B. Keller and J. S. Papadakis, Lecture Notes in Physics, vol. 70, Springer-Verlag, Heidelberg, 1977.
5. D. Lee, G. Botseas, and J. S. Papadakis, "Finite-Difference Solutions to the Parabolic Wave Equation," Journal of the Acoustical Society of America, vol. 70, no. 3, 1981, pp. 795-800.
6. D. Lee and J. S. Papadakis, "Numerical Solutions for the Parabolic Wave Equation: An Ordinary-Differential-Equation Approach," Journal of the Acoustical Society of America, vol. 68, 1980, pp. 1482-1488.
7. B. Carnahan, H. A. Luther, and J. O. Wikes, Applied Numerical Methods, John Wiley and Sons, Inc., NY, 1969.
8. S. T. McDaniel and D. Lee, "A Finite-Difference Treatment of Interface Conditions for the Parabolic Wave Equation: The Horizontal Interface," Journal of the Acoustical Society of America, vol. 71, no. 4, 1982, pp. 855-859.
9. D. Lee and G. Botseas, IFD: An Implicit Finite-Difference Computer Model for Solving the Parabolic Equation, NUSC Technical Report 6659, Naval Underwater Systems Center, New London, CT, 27 May 1982.
10. K. E. Gilbert, "A Finite Element Method for the Parabolic Wave Equation," NORDA Parabolic Equation Workshop, edited by J. A. Davis, D. White, and R. C. Cavanagh, TN-143, Naval Ocean Research and Development Activity, Bay St. Louis, MS, 1982.
11. R. Green, "High Angle PE," NORDA Parabolic Equation Workshop, edited by J. A. Davis, D. White, and R. C. Cavanagh, TN-143, Naval Ocean Research and Development Activity, Bay St. Louis, MS, 1982.

12. D. Lee and K. E. Gilbert, "Recent Progress in Modeling Bottom-Interacting Sound Propagation With Parabolic Equations," Oceans 82, 1982, pp. 172-177.
13. K. E. Gilbert, D. Lee, and G. Botseas, "Theory, Development, and Implementation of a Wide-Angle Parabolic Equation," Journal of the Acoustical Society of America (in preparation).
14. J. F. Claerbout, Fundamentals of Geophysical Data Processing, McGraw-Hill Book Co., Inc., NY, 1976, pp. 206-207.
15. A. J. Berkhouit, "Wave Field Extrapolation Techniques in Seismic Migration, A Tutorial," Geophysics, vol. 46, no. 12, 1981, pp. 1638-1656.
16. NORDA Parabolic Equation Workshop, edited by J. A. Davis, D. White, and R. C. Cavanagh, TN-143, Naval Ocean Research and Development Activity, Bay St. Louis, MS, 1982.
17. H. W. Kutschale, "Fast Field Program," NORDA Parabolic Equation Workshop, edited by J. A. Davis, D. White, and R. C. Cavanagh, TN-143, Naval Ocean Research and Development Activity, Bay St. Louis, MS, 1982.

INITIAL DISTRIBUTION LIST

Addressee	No. of Copies
ONR, ONR-100, -102, -200, -220, -400, -422, -425AC	7
CNO, OP-952	1
NRL	1
OCEANAV	1
NAVOCEANO	2
NAVSEASYSCOM, SEA-63D, -63R, -63R-1, -63R-13	4
NAVAIRDEVcen	1
NOSC, Code 8302	1
NAVPGSCOL	1
ARL, PENN STATE, STATE COLLEGE	1
Admiralty Underwater Weapons Estab., England (Dr. Roy Levers)	1
Defence Research Estab. Atlantic, Dartmouth, N.S., Canada (Dr. D. Chapman)	1
DREP, Canada (Dr. N. R. Chapman)	1
Dept. of Defence, Weapon Systems Research Lab., Adelaide, South Australia (Dr. D. J. Kewley)	1
NORDA (Dr. K. E. Gilbert)	50
NOAA/OAL (Dr. D. Palmer, Dr. John Tsai)	2
SACLANT ASW Research Center, NY (Dr. F. B. Jensen)	1
Iowa State University, IA (Dr. James Coronis)	1
APL, Johns Hopkins University, MD (Dr. R. F. Henrick)	1
NAVPGSCOL (Prof. Calvin R. Dunlap, LT L. E. Jaeger)	2
University of New Orleans, LA (Prof. J. Murphy)	1
Rensselaer Polytechnical Institute, NY (Prof. W. L. Siegmann)	1
ARL, UNIV OF TEXAS (Prof. R. Koch, Susan Payne)	2
Yale University, CT (Prof. M. H. Schultz)	1
Forschungsanstalt der Bundeswehr Fuer Wasserschall - und Geophysik, Germany (Prof. G. Ziehm)	1
UNIV OF TENNESSEE (Dr. V. Doogalis)	1
UNIV OF MIAMI, FL (Prof. F. D. Tappert)	1
Universite De Sherbrooke, Canada (Dr. A. H. Bokhari)	1
TRW, CA (F. E. Fendell)	1
FLOPETROL, SCHLUMBERGER, France (C. C. Speake)	1
UNIV OF RHODE ISLAND (Prof. J. S. Papadakis)	1

END

FILMED

3-86

DTIC